

Electrical Characteristics of Al₂O₃/InSb MOSCAPs and the Effect of Postdeposition Annealing Temperatures

Hai Dang Trinh, Yueh Chin Lin, Edward Yi Chang, *Senior Member, IEEE*, Ching-Ting Lee, *Fellow, IEEE*, Shin-Yuan Wang, Hong Quan Nguyen, Yu Sheng Chiu, Quang Ho Luc, Hui-Chen Chang, Chun-Hsiung Lin, Simon Jang, and Carlos H. Diaz, *Fellow, IEEE*

Abstract—The characteristics of Al₂O₃/InSb MOSCAPs processed with different postdeposition annealing (PDA) temperatures are investigated. X-ray photoelectron spectroscopy analysis shows a significant reduction of InSb-oxides after HCl plus trimethyl aluminum treatment and oxide deposition. Multifrequency capacitance-voltage (*C*-*V*) characteristics exhibit low-frequency and asymmetrical *C*-*V* behaviors, in which capacitance in the InSb conduction band side is lower than in the valence band side. The electrical properties of the MOSCAPs are sensitive to PDA temperature and degraded significantly at PDA temperature >300 °C. This degradation is closely related to the diffusion of In, Sb into Al₂O₃ as indicated by transmission electron microscopy analyses.

Index Terms—Al₂O₃, asymmetrical *C*-*V*, atomic layer deposition (ALD), InSb, MOS, post deposition annealing (PDA).

I. INTRODUCTION

BESIDES the use in infrared imaging systems, high carrier mobility, narrow-gap InSb has drawn attention for its potential in extremely high-speed, low-power CMOS devices application such as nanowire, quantum well (QW) or band-to-band tunneling (T) field-effect-transistors (FETs). Among III-V compounds, InSb has the highest electron

mobility of $7.7 \times 10^4 \text{ cm}^2\text{V}^{-1}\text{s}^{-1}$ and hole mobility of $840 \text{ cm}^2\text{V}^{-1}\text{s}^{-1}$ [1], which promise of both n- and p-channel high-performance transistors. InSb-based QWFETs demonstrated very-high speed performance at low supply voltage (0.5 V) for both n- and p-channels devices [2], [3]. The integration of InSb on Si for MOS devices application was also reported [4]. For both infrared and CMOS applications, the deposition of dielectric layer with good quality interfacial properties is essential for the effective performance of devices. Several methods such as anodic oxidation, plasma-enhanced chemical vapor deposition (PECVD), remote PECVD, and low-temperature chemical vapor deposition are used to deposit the insulator/oxide layer on InSb for studying. However, the study of InSb MOS capacitors (MOSCAPs) using atomic layer deposition (ALD) oxide is still seldom [4]–[7]. The ALD method is well known to be a robust and manufacturable process, which is promising for manufacturing of CMOS technology. Because InSb has low thermal budget [1], the electrical characteristics of the ALD oxide/InSb MOSCAPs are sensitive to thermal processes. In this paper, the electrical properties of ALD Al₂O₃/InSb MOSCAPs and their dependent on postdeposition annealing (PDA) temperatures are studied. The multifrequency asymmetrical *C*-*V* behavior of Al₂O₃/n-InSb MOSCAPs due to the low density of state (DOS) in InSb conduction band is experimentally observed in this paper. The out diffusion of In, Sb atoms into Al₂O₃ is found to be the major effect on the electrical degradation of the MOSCAPs such as hysteresis, frequency dispersion, *C*-*V* modulation, *C*-*V* stretch-out, and interface density of states D_{it} .

II. MATERIALS AND EXPERIMENT

Wafers used in this research are InSb (100) undoped substrate, naturally n-type behavior with donor concentration of $2.2 \times 10^{16} \text{ cm}^{-3}$ at room temperature, determined by Hall measurement. The wafers are initially degreased by rinsing in acetone and isopropanol for 2 min each. The samples are dipped in the diluted HCl 4% solution for 2 min, rising in deionized water, and blown dry by N₂ gas. The samples are then loaded into ALD chamber (Cambridge NanoTech Fiji 202 DSC) within 5 min after cleaning. In ALD chamber, the samples are precleaned by using ten pulses of trimethyl aluminum (TMA)/Ar [8]–[10] before the deposition of 85 cycles

Manuscript received December 17, 2012; revised February 2, 2013; accepted March 15, 2013. Date of current version April 18, 2013. This work was supported by the Taiwan National Science Council under Contract 101-2923-E-009-002-MY3 and Contract 99-2221-E-164-MY3.

H. D. Trinh was with the Department of Materials Science and Engineering, National Chiao Tung University, Hsinchu 300, Taiwan. He is currently with the Manufacturing Company Limited, Hsinchu Science Park, Hsinchu 300, Taiwan (e-mail: trindhaidang@gmail.com).

Y. C. Lin, H. Q. Nguyen, Y. S. Chiu, and Q. H. Luc are with the Department of Materials Science and Engineering, National Chiao Tung University, Hsinchu 300, Taiwan (e-mail: nctulin@yahoo.com.tw; quansply@yahoo.com; laurance0319@yahoo.com.tw; lucquangho@gmail.com).

E. Y. Chang is with the Department of Materials Science and Engineering and the Department of Electronic Engineering, National Chiao Tung University, Hsinchu 300, Taiwan (e-mail: edc@mail.nctu.edu.tw).

C.-T. Lee is with Department of Electrical Engineering, National Cheng Kung University, 01 University Road, Tainan 701, Taiwan (e-mail: ctlee@ee.ncku.edu.tw).

S.-Y. Wang is with the Department of Electronic Engineering, National Chiao Tung University, Hsinchu 300, Taiwan (e-mail: leoplct@gmail.com).

H.-C. Chang, C.-H. Lin, S. M. Jang, and C. H. Diaz are with the Taiwan Semiconductor Manufacturing Company Limited, Hsinchu Science Park, Hsinchu 300, Taiwan (e-mail: changhcm@tsmc.com; linczzz@tsmc.com; smjang@tsmc.com; chdiaz@tsmc.com).

Color versions of one or more of the figures in this paper are available online at <http://ieeexplore.ieee.org>.

Digital Object Identifier 10.1109/TEDE.2013.2254119

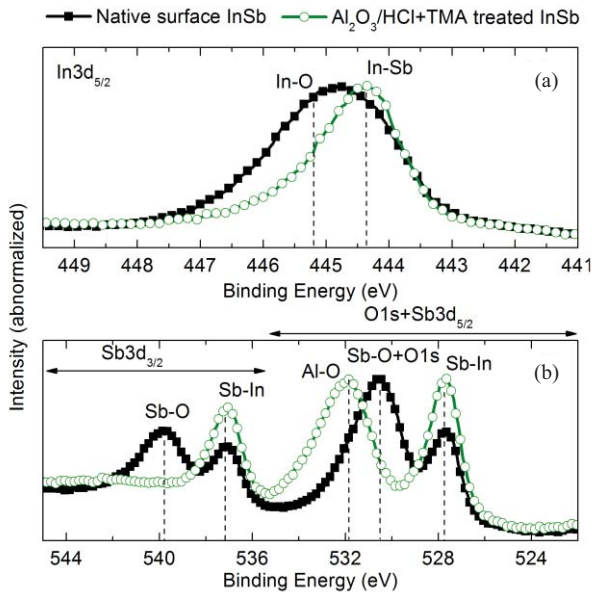


Fig. 1. (a) In $3d_{5/2}$ and (b) Sb $3d$ plus O $1s$ XPS spectra of native InSb surface and 1.5-nm $\text{Al}_2\text{O}_3/\text{InSb}$ interface.

(~ 7.5 nm) Al_2O_3 at 250°C , using TMA and H_2O as precursors. The HCl plus TMA treatment is proved to improve effectively $\text{Al}_2\text{O}_3/\text{InAs}$ interface [8], [9]. The effect of TMA treatment in the reduction of InSb native oxides is also reported [5]. The samples are PDA at different temperatures of 300°C , 350°C , and 400°C in N_2 for 30 s. Ni/Au metal gate is formed via photolithography/e-beam evaporation/lift-off process. Finally, Au/Ge/Ni/Au is deposited for backside ohmic contact followed by postmetal annealing at 250°C in N_2 for 30 s. The multifrequency $C-V$ is measured by an HP4284A LCR meter. The quasistatic $C-V$ (QSCV) curves are performed using an Agilent B1500A semiconductor device analyzer. The chemical and structural properties of $\text{Al}_2\text{O}_3/\text{InSb}$ interface are studied by X-ray photoelectron spectroscopy (XPS) measurement using a commercial Microlab 350 XPS system and transmission electron microscopy (TEM) using a Philips Tecnai F-20 microscope with energy-dispersive X-ray spectroscopy (EDS) analysis.

III. RESULTS AND DISCUSSION

Fig. 1 shows In $3d_{5/2}$ and Sb $3d$ plus O $1s$ XPS spectra of native InSb surface and the 1.5-nm ALD $\text{Al}_2\text{O}_3/\text{HCl}$ plus TMA-treated InSb interface. The O $1s$ peak overlapped with the Sb $3d_{5/2}$ -related oxides peak. After surface treatment and oxide deposition, In-oxides are reduced significantly as shown in In $3d_{5/2}$ spectra [Fig. 1(a)]. The Sb $3d_{3/2}$ spectra in Fig. 1(b) show the reduction of Sb-related oxides below the XPS detection level. The O $1s$ plus oxidized Sb $3d_{5/2}$ peak originally assigned to O-Sb and O-In bonds shifted to higher binding energy, which is mostly attributed to Al-O bonds. Similar O $1s$ peak position corresponding to Al-O bonds is also obtained by *in situ* XPS measurement of 1-nm ALD $\text{Al}_2\text{O}_3/\text{ammonium sulfide}$ -treated InSb [11].

Fig. 2(a) shows the typical $C-V$ behavior of the MOSCAPs at frequency of 1 MHz. The observed low-frequency $C-V$ response at high frequency of 1 MHz is due to the high intrinsic carrier density n_i in InSb material [$n_i \sim 2 \times 10^{16} \text{ cm}^{-3}$ at

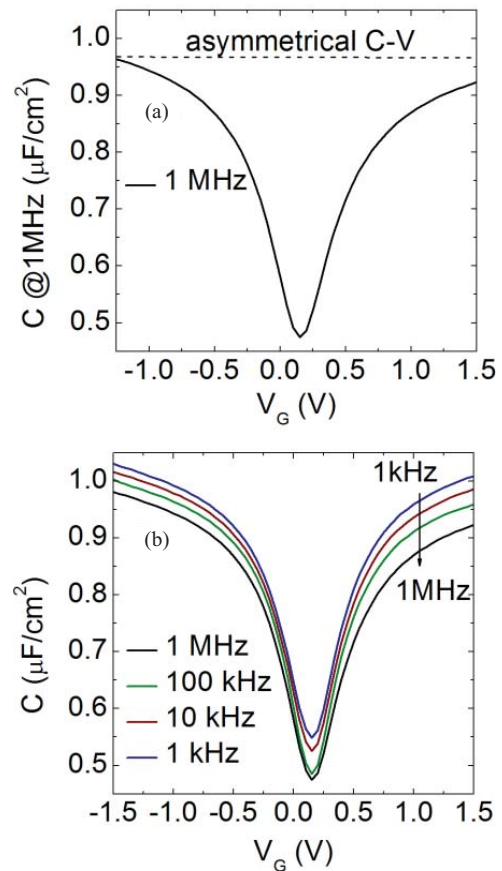


Fig. 2. (a) Typical low-frequency asymmetrical $C-V$ response at 1 MHz. (b) Typical multifrequency $C-V$ responses of $\text{Al}_2\text{O}_3/\text{InSb}$ MOSCAP structure.

TABLE I
PARAMETERS OF InSb USED IN (1) [1]

t_{Tn} (s)	t_{Tp} (s)	N_D (cm^{-3})	n_i (cm^{-3})	N_C (cm^{-3})	N_V (cm^{-3})
5×10^{-8}	5×10^{-8}	2.2×10^{16}	2×10^{16}	4.2×10^{16}	7.3×10^{18}

room temperature (RT)] [1]. The relation between n_i and the minority carrier response time τ_R is given by [10]

$$\tau_R = \frac{1}{\sqrt{2}} \frac{N_D}{n_i} \tau_T \left(1 - \frac{v_T}{u_B}\right)^{1/2} \quad (1)$$

where N_D is donor doping density, $\tau_T = \sqrt{\tau_{Tn}\tau_{Tp}}$ (τ_{Tn} and τ_{Tp} are bulk electron and hole life times), v_T and u_B are potentials above the intrinsic level of bulk trap and Fermi levels in InSb [9]. By taking the parameters in Table I [1], the value of τ_R in InSb estimated by (1) is of 3.9×10^{-8} s at room temperature. This very short response time would allow minority carriers to respond to such high-frequency ac signal as 1 MHz.

The asymmetrical $C-V$ curve, in which the capacitance on the InSb conduction band side is lower than on the valence band side, is also observed obviously in Fig. 2(a). To our knowledge, this observation is first time witnessed by experimental high-frequency $C-V$ measurement. The observation at high frequency of 1 MHz is due to the observation of low-frequency $C-V$ response in InSb-based MOSCAPs as

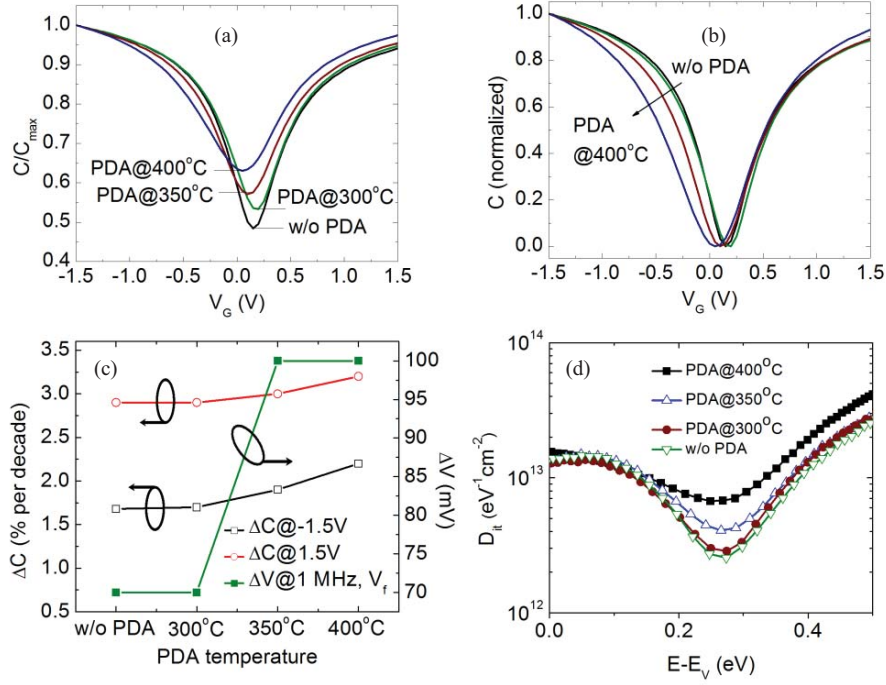


Fig. 3. (a) $C/C_{\max} - V$. (b) Normalized $C-V$ characteristics at 1 MHz of the Al₂O₃/InSb MOSCAPs with different PDA temperatures. (c) Frequency dispersion, hysteresis. (d) Interface trap profiles of the MOSCAPs increase significantly at PDA temperature greater or equal to 350 °C.

discussed above and a very low DOS in InSb conduction band (N_C). At RT, the value of N_C is $4.2 \times 10^{16} \text{ cm}^{-3}$, which is 170-fold lower than N_V ($7.3 \times 10^{18} \text{ cm}^{-3}$) [1]. This low value of N_C would lead to the semiconductor capacitance C_S could not be very large compared with oxide capacitance C_{ox} , and thus results in lower the total capacitance C_{tot} in the conduction band side according to the following equation [12]:

$$C_{\text{tot}} = C_{\text{ox}} \left(1 + \frac{C_{\text{ox}}}{C_S + C_{\text{tr}}} \right)^{-1} \quad (2)$$

where C_{tr} is capacitance by the traps at/near Al₂O₃/InSb interface.

The typical multifrequency $C-V$ response of Al₂O₃/InSb MOSCAPs is shown in Fig. 2(b). At low frequency, the asymmetrical $C-V$ behavior becomes less significant that implies the increase of the contribution of C_{tr} to the C_{tot} with the decrease of the measuring frequency [see (2)]. For narrow gap semiconductor as InSb, the interface traps response time is so short that it can follow the ac signal with frequency in the range 1 kHz to 1 MHz [13]. In this context, the increase of C_{tr} with the decrease of measuring frequency might come from the interaction of traps located inside oxide (called border traps) with conduction band electrons via tunneling [13].

Fig. 3 shows the comparison of samples underwent various PDA temperatures. The $C/C_{\max}-V$ responses at 1 MHz of samples are shown in Fig. 3(a). The modulation of $C-V$ curves is less significant with the increase of the PDA temperatures. Fig. 3(b) and (c) shows the increase significantly of $C-V$ stretch-out, frequency dispersion, and hysteresis when the PDA temperature is greater than or equal to 350 °C. The $C-V$ stretchout is caused by the slow interface/border traps that could not follow the ac signal but do follow the dc bias sweep [14]. The degradation of $C-V$ stretchout is significant

in the negative gate bias side [Fig. 3(b)] shows a noticeable increase of the donor-like interface/border traps at the PDA temperature of 350 °C and above. To quantify the degradation, the interface traps are extracted by low-frequency $C-V$ fitting method by self-consistent solution of Schrodinger–Poisson equations, similar to the approach in [15] and [16]. Initially, the semiconductor capacitance C_S is extracted by solving the Schrodinger–Poisson equations of the Al₂O₃/InSb ideal MOS structure (without interface density). The capacitance due to interface traps of the real MOS structure (C_{it}) is calculated by from the following equation [17]:

$$C_{\text{it}} = \frac{C_{\text{ox}} C_{\text{mes}}}{C_{\text{ox}} - C_{\text{mes}}} - C_S \quad (3)$$

where, C_{ox} is the oxide capacitance and C_{mes} is experimental QSCV data. From this value, the simulated $C-V$ curve is extracted and compared again with the experimental $C-V$ curve. Some parameters of the MOS structures such as flat band voltage (V_{fb}) and charge neutral level (E_{CNL}) are modulated by the simulation and the D_{it} profile is extracted when the best fit between simulating and experimental $C-V$ is occurred. The traps energy level E is defined from the equation [15], [16]

$$E - E_C = E_g + E_F - q\phi_s \quad (4)$$

where E_C , E_g , and E_F are conduction band minimum level, band gap, and Fermi level in InSb, respectively, and ϕ_s is surface potential. The surface potential is determined from the gate bias V_g given by

$$\phi_s = V_g - V_{\text{fb}} + \frac{Q_s + Q_{\text{it}}}{C_{\text{ox}}} \quad (5)$$

where Q_s and Q_{it} are the semiconductor charge and interface trap charge, respectively. The D_{it} profiles are similar for the

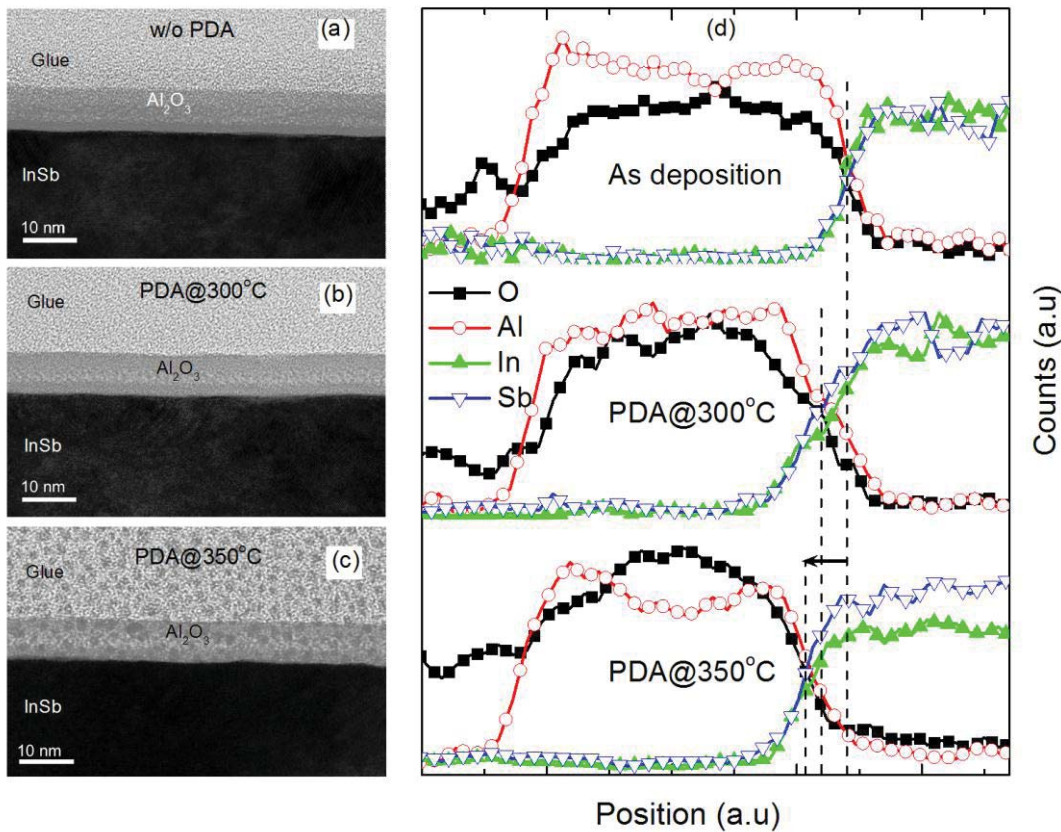


Fig. 4. TEM images of the $\text{Al}_2\text{O}_3/\text{InSb}$ structures. (a) After oxide deposition. (b) PDA at 300°C , 30 s. (c) PDA at 350°C , 30 s. (d) EDS spectra of the samples.

samples without PDA and PDA at 300°C with minimum value of $2.55 \times 10^{12} \text{ eV}^{-1}\text{cm}^{-2}$ at trap position $E-E_V = 0.275 \text{ eV}$ as shown in Fig. 3(d). Simultaneously, the minimum of D_{it} levels of the samples which went through PDA at 350 and 400°C increases significantly with increasing PDA temperatures.

The high-resolution transmission electron microscopy analyses of $7.5\text{-nm Al}_2\text{O}_3/\text{InSb}$ as dep, PDA at 300°C and 350°C are shown in Fig. 4 (the TEM figure of the sample PDA at 350°C is the spotted through the use of Pt for preventing the sample's damage). From the high-resolution cross-sectional TEM image in Fig. 4(a), it is clearly shown that the as deposited sample exhibits a double-layer gate oxide with thickness of $1.5 \text{ nm}/6 \text{ nm}$. The 1.5-nm layer is attributed to the out diffusion of In, Sb into Al_2O_3 during the 1 h suffered at 250°C oxide deposition process. The out-diffusion layer increases with the increasing of PDA temperatures as indicated in Fig. 4(a)–(c). The EDS analysis of the samples shown in Fig. 4(d) also indicates the increase of In, Sb out-diffusion into Al_2O_3 with the increasing of PDA temperatures. This strong out-diffusion would result in the degradation of $\text{Al}_2\text{O}_3/\text{InSb}$ interface as well as Al_2O_3 oxide itself, which leads to the degradation of the electrical properties of the MOSCAPs as discussed above.

IV. CONCLUSION

In conclusion, we discussed the electrical properties of $\text{Al}_2\text{O}_3/\text{InSb}$ MOSCAPs and their dependent on PDA

temperature. The low-frequency asymmetrical $C-V$ behavior was experimentally observed at high-frequency $C-V$ measurement because of the short minority carrier response time and low DOS in InSb conduction bandgap. When the PDA temperature was increased to 350°C and above, the electrical properties of the MOSCAPs degraded significantly. This degradation was due to the strong out diffusion of In, Sb atoms into the Al_2O_3 oxide layer with the increase of PDA temperature proved by TEM and EDS analyses.

REFERENCES

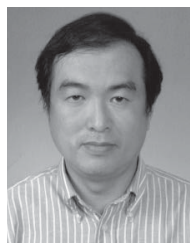
- [1] M. Levinshtein, S. Rumyantsev, and M. Shur, *Handbook Series on Semiconductor Parameters*. Singapore: World Scientific, 1996.
- [2] S. Datta, T. Ashley, J. Brask, L. Buckle, M. Doczy, M. Emeny, D. Hayes, K. Hilton, R. Jefferies, T. Martin, T. J. Phillips, D. Wallis, P. Wilding, and R. Chau, "85 nm Gate length enhancement and depletion mode InSb quantum well transistors for ultra high speed and very low power digital logic applications," in *Proc. IEEE Int. IEDM Tech. Dig. Electron Devices Meeting*, Dec. 2005, pp. 763–766.
- [3] M. Radosavljevic, T. Ashley, A. Andreev, S. D. Coomber, G. Dewey, M. T. Emeny, M. Fearn, D. G. Hayes, K. P. Hilton, M. K. Hudait, R. Jefferies, T. Martin, R. Pillarisetty, W. Rachmady, T. Rakshit, S. J. Smith, M. J. Uren, D. J. Wallis, P. J. Wilding, and R. Chau, "High-performance 40 nm gate length InSb p-channel compressively strained quantum well field effect transistors for low-power ($V_{CC}=0.5 \text{ V}$) logic applications," in *Proc. IEEE Int. IEDM Electron Dev. Meeting*, Dec. 2008, pp. 727–730.
- [4] A. Kadoda, T. Iwasugi, K. Nakatani, K. Nakayama, M. Mori, K. Maezawa, E. Miyazaki, and T. Mizutani, "Characterization of $\text{Al}_2\text{O}_3/\text{InSb}/\text{Si}$ MOS diodes having various InSb thicknesses grown on Si(1 1 1) substrates," *Semicond. Sci. Technol.*, vol. 27, no. 4, pp. 045007-1–045007-6, Feb. 2012.

- [5] C. H. Hou, M. C. Chen, C. H. Chang, T. B. Wu, C. D. Chiang, and J. J. Luo, "Effects of surface treatments on interfacial self-cleaning in atomic layer deposition of Al₂O₃ on InSb," *J. Electrochem. Soc.*, vol. 155, no. 9, pp. G180–G183, Jul. 2008.
- [6] H.-Y. Chou, V. V. Afanas'ev, M. Houssa, A. Stesmans, L. Dong, and P. D. Ye, "Electron band alignment at the interface of (100)InSb with atomic-layer deposited Al₂O₃," *Appl. Phys. Lett.*, vol. 101, no. 8, pp. 082114-1–082114-3, Aug. 2012.
- [7] H.-S. Kim, I. Ok, M. Zhang, F. Zhu, S. Park, J. Yum, H. Zhao, J. C. Lee, P. Majhi, N. Goel, W. Tsai, C. K. Gaspe, and M. B. Santos, "A study of metal-oxide-semiconductor capacitors on GaAs, In_{0.53}Ga_{0.47}As, InAs, and InSb substrates using a germanium interfacial passivation layer," *Appl. Phys. Lett.*, vol. 93, no. 6, pp. 062111-1–062111-3, Aug. 2008.
- [8] H.-D. Trinh, E. Y. Chang, Y.-Y. Wong, C.-C. Yu, C.-Y. Chang, Y.-C. Lin, H.-Q. Nguyen, and B.-T. Tran, "Effects of wet chemical and trimethyl aluminum treatments on the interface properties in atomic layer deposition of Al₂O₃ on InAs," *Jpn. J. Appl. Phys.*, vol. 49, no. 11, pp. 111201-1–111201-4, Nov. 2010.
- [9] H. D. Trinh, G. Brammertz, E. Y. Chang, C. I. Kuo, C. Y. Lu, Y. C. Lin, H. Q. Nguyen, Y. Y. Wong, B. T. Tran, K. Kakushima, and H. Iwai, "Electrical characterization of Al₂O₃/n-InAs metal-oxide-semiconductor capacitors with various surface treatments," *IEEE Electron Device Lett.*, vol. 32, no. 6, pp. 752–754, May 2011.
- [10] H. D. Trinh, E. Y. Chang, P. W. Wu, Y. Y. Wong, C. T. Chang, Y. F. Hsieh, C. C. Yu, H. Q. Nguyen, Y. C. Lin, K. L. Lin, and M. K. Hudait, "The influences of surface treatment and gas annealing conditions on the inversion behaviors of the atomic-layer-deposition Al₂O₃/n-In_{0.53}Ga_{0.47}As metal-oxide semiconductor capacitor," *Appl. Phys. Lett.* vol. 97, no. 4, pp. 042903-1–042903-3, Jul. 2010.
- [11] D. M. Zhernokletov, H. Dong, B. Brennan, J. Kim, and R. M. Wallace, "In situ X-ray photoelectron spectroscopy characterization of Al₂O₃/InSb interface evolution from atomic layer deposition," *Appl. Surf. Sci.*, vol. 258, no. 14, pp. 5522–5525, Feb. 2012.
- [12] E. H. Nicollian and J. R. Brews, *Metal Oxide Semiconductor Physics and Technology*. New York, NY, USA: Wiley, 1982.
- [13] Y. Yu, W. Lingquan, Y. Bo, S. Byungha, A. Jaesoo, P. C. McIntyre, P. M. Asbeck, M. J. W. Rodwell, and T. Yuan, "A distributed model for border traps in Al₂O₃-InGaAs MOS devices," *IEEE Electron Device Lett.*, vol. 32, no. 4, pp. 485–487, Apr. 2011.
- [14] C.-W. Cheng, G. Apostolopoulos, and E. A. Fitzgerald, "The effect of interface processing on the distribution of interfacial defect states and the C-V characteristics of III-V metal-oxide-semiconductor field effect transistors," *J. Appl. Phys.*, vol. 102, no. 2, pp. 023714-1–023714-8, Jan. 2011.
- [15] M. M. Satter, A. E. Islam, D. Varghese, M. A. Alam, and A. Haque, "A self-consistent algorithm to extract interface trap states of MOS devices on alternative high-mobility substrates," *Solid-State Electron.*, vol. 56, no. 1, pp. 141–147, Feb. 2011.
- [16] H. Q. Nguyen, H. D. Trinh, E. Y. Chang, C. T. Lee, S. Y. Wang, H. W. Yu, C. H. Hsu, and C. L. Nguyen, "In_{0.5}Ga_{0.5}As-based metal-oxide-semiconductor capacitor on GaAs substrate using metal-organic chemical vapor deposition," *IEEE Trans. Electron Devices*, vol. 60, no. 1, pp. 235–240, Jan. 2013.
- [17] D. K. Schroder, *Semiconductor Material and Device Characterization*. New York, NY, USA: Wiley, 2006.



Yueh Chin Lin received the Ph.D. degree from the National Chiao Tung University (NCTU), Hsinchu, Taiwan, in 2000.

He is currently a Post-Doctoral Researcher with the Compound Semiconductor Device Laboratory, Department of Materials Science and Engineering, NCTU.



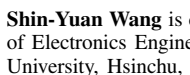
Edward Yi Chang (S'85–M'85–SM'04) received the Ph.D. degree from the University of Minnesota, Minneapolis, MN, USA, in 1985.

He is currently the Dean of Office of Research and Development, National Chiao Tung University, Hsinchu, Taiwan.



Ching-Ting Lee (F'09) received the Ph.D. degree from Carnegie-Mellon University, Pittsburgh, PA, USA, in 1982.

He is currently a Professor with the Institute of Microelectronics, Department of Electrical Engineering, National Cheng Kung University, Tainan, Taiwan.

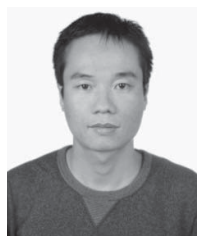


Shin-Yuan Wang is currently pursuing the Ph.D. degree with the Department of Electronics Engineering and Institute of Electronics, National Chiao-Tung University, Hsinchu, Taiwan.



Hong Quan Nguyen received the Ph.D. degree in materials science and engineering from National Chiao Tung University (NCTU), Hsinchu, Taiwan, in 2012.

He is currently a Post-Doctoral Researcher with the Department of Materials Science and Engineering, NCTU.



Hai Dang Trinh received the Ph.D. degree from National Chiao Tung University, Hsinchu, Taiwan, in 2011.

He is currently with the Specialty Module Division, Taiwan Manufacturing Company Limited, Hsinchu Science Park, Hsinchu.

Yu Sheng Chiu is currently pursuing the Ph.D. degree with the Department of Materials Science and Engineering, National Chiao Tung University, Hsinchu, Taiwan.



Quang Ho Luc is currently pursuing the Ph. D. degree with the Department of Materials Science and Engineering, National Chiao Tung University, Hsinchu, Taiwan.

Simon Jang currently a Director of Advanced Technology Module Division, Taiwan Semiconductor Manufacturing Company (TSMC), Hsinchu Science Park, Hsinchu, Taiwan.

Hui-Chen Chang is currently a Senior Manager with the Advanced Technology Module Division, Taiwan Semiconductor Manufacturing Company, Hsinchu Science Park, Hsinchu.



Carlos H. Diaz (F'08) received the Ph.D. degree in electrical engineering from the University of Illinois at Urbana-Champaign, Urbana, IL, USA.

He is currently the Director of Advanced Device Technology, Taiwan Semiconductor Manufacturing Company, Hsinchu Science Park, Hsinchu, Taiwan.



Chun-Hsiung Lin received the Ph.D. degree in materials science and engineering from the University of Illinois at Urbana-Champaign, Urbana, IL, USA, in 2000.

He is currently a Manager with Taiwan Semiconductor Manufacturing Company, Hsinchu Science Park, Hsinchu, Taiwan.